-RESEARCH PAPER-

International Journal of Mining and Geo-Engineering

IJMGE

IJMGE 58-4 (2024) 439-444

DOI: 10.22059/IJMGE.2024.379874.595183

Block caving underground mining technique under an existing open-pit mine: Investigating the effect of undercut depth on crown pillar thickness

Behnam Alipenhani [a,*], Erfan Amini [b], Hassan Bakhshandeh Amnieh [a], and Abbas Majdi [a]

[a] *School of Mining Engineering, College of Engineering, University of Tehran, Tehran, Iran.*

Article History:

Received: 24 July 2024.

Revised: 31 October 2024.

Accepted: 18 November 2024.

ABSTRACT

Block caving method is the most suitable underground mining method for metal deposits that have reached their transition depth. The stability of the pit floor and slopes of these mines is critical to ensure safety and prevent damage to surface infrastructure. In this paper, the process of block caving under the open pit mine is modeled by numerical simulation using Phase 2 software. The effect of undercut depth on the caving height and the thickness of the remaining crown pillar under the pit was investigated. The undercut was modeled at 200, 600, and 1000 meters below the pit floor. The results show that the height of the caving increases with increasing depth of the undercut. The maximum cave span also increases with the increment in depth. Also, as the depth increases from 200 to 600 meters, the thickness of the crown pillar increases five-fold, whereas by increasing the depth of undercutting from 600 to 1000 meters, the thickness of the crown pillar doubles. In addition, the ratio of the crown pillar thickness to the maximum caving span decreases as the depth of undercut increases. At depth of 200 meters to 600 meters, the mentioned ratio decreases severely; however, for depths between 600 meters and 1000 meters, the ratio decreases gradually.

Keywords: *Block caving, Open pit, Transition depth, Numerical modeling.*

1. Introduction

Globally, the demand for minerals is increasing. Conversely, surface resources are declining. Many large and worldwide mines have changed their exploitation method from open-pit mining to block caving method, as the depth of the pit increases and it becomes uneconomical. Among the advantages of the block caving method, we can mention its low cost and high production rate; therefore, low-grade deposits can be mined using this method [1–4].

Block caving mining under an existing open-pit mine can cause the instability of the open-pit mine slopes, and excessive settlement in the pit floor and ground surface. Therefore, a crown pillar should remain under the open-pit floor to control these issues. Numerical modelling, physical modelling, and analytical methods have been used to investigate the mechanism of the impact of block caving on the stability of the upper open-pit mine. A summary of these researches is given in Table 1.

According to Table 1, researchers have conducted prominent studies in the prediction of pit subsidence behavior under the influence of block caving. However, this is a challenging issue in mining engineering. In this paper, the combined effect of the undercut depth and undercutting sequence on the thickness of the crown pillar under an existing open-pit mine, regarding rock mass strength parameters, has been investigated.

2. Block Caving Method

Figure 1 shows an overview of the block caving method. In this method, an undercut is excavated in the entire ore body or in a block whose dimensions are almost equal to the dimensions of the ore body [15]. After excavation of the undercut, some parts of the caved ore are drawn through the draw point which has been designed in advance to provide the necessary space for the collapse of the upper ores. As the broken ore continues to be drawn, the host rocks are caved and consequently, the ground subsidence occurs, the primary caving propagates upward in the entire deposit [16,17]. The effect of mechanical and geometrical parameters, such as joint set number, joint spacing, joint inclination angle, joint surface friction angle, and undercut depth on the caving span, height of the caving, and rock mass cavability were investigated by Alipenhani et al. [18–21] using physical and numerical modelling as well as employing Gene Expression Programming and Artificial Neural Networks to create heuristic models.

Some of the main reasons for transitioning open-pit mines into block and panel caving mines are [22]:

- It is not economical to continue open-pit mines.
- Uncertainty about the stability and safety of the high slopes in open-pit mines.
- Harmful environmental effects of the open-pit mines development.
- Lower operational cost and greater production capacity of block and panel caving methods compared to other underground (non-selective) mass extraction methods.

Figure 2 demonstrates the schematic representation of the Chuquicamata open-pit mine, in which a block caving mine has been implemented below that.

3. Numerical Modelling

In this paper, three models were generated and analysed. In the first model, the slope height is 200 meters, and the width of the undercut is 100 meters. The undercut is excavated in 10 steps. The difference

* Corresponding author: *E-mail address:* b.alipenhani@ut.ac.ir (B. Alipenhani).

Table 1. A brief history of the researches on the impact of underground mining on the stability of upper open-pit mine.

Model type	References	Purpose and application
Empirical	Woo *et al.* [5]	Using an empirical method to investigate and describe open-pit subsidence associated with block caving mining
Physical modelling	Ren *et al.* [6]	Physical modelling to predict the expansion of the caving zone caused by the underground caving method
	Yang *et al.* [7]	3D physical modelling to investigate the effects of joint sets on the open-pit floor subsidence mechanism and comparing the results with numerical simulation
Numerical modelling	Flores and Karzulovic [8]	An open-pit floor subsidence analysis related to open-pit block caving interaction using FLAC2D numerical simulation software and a limit equilibrium technique
	Eberhardt *et al.* [9]	Analysis of cave-induced slope deformations using FLAC2D and UDEC. The modelling approach, as well as the geometry of the discontinuity network, can affect the magnitude and shape of the subsidence profile.
	Elmo *et al.* [10]	Modelling open-pit block caving interaction using FEM/DEM-DFN methods
	Beck *et al.* [11]	Using ABAQUS software to analyze the interaction between open-pit mines and block caving through plastic energy and strain
	Xu *et al.* [12]	Using numerical modelling with 3DEC software to predict damage extension of Yanqianshan iron mine's pit slope caused by underground mining
	Svarttjern *et al.* [13]	A numerical modelling by using PFC2D to analyze the footwall damage in Kiirunavaara mine caused by subsurface caving
	Tegachouang *et al.* [14]	Analysis of the effects of the underground block caving mining on the stability of an adjacent open-pit mine

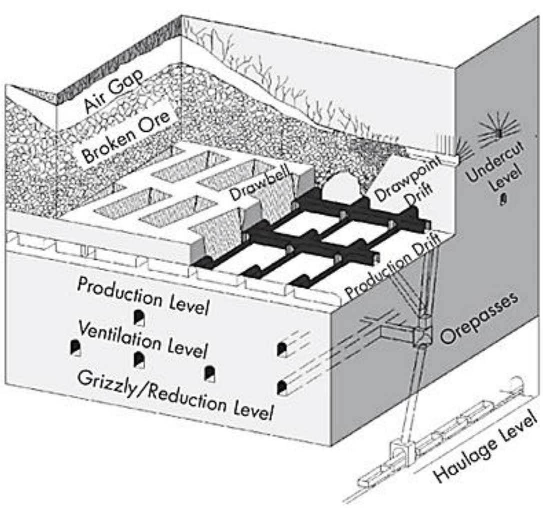

Figure 1. A schematic image of a block caving mine [15].

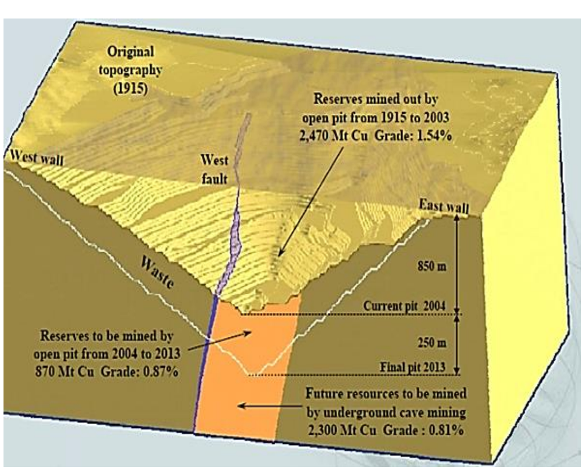

Figure 2. The schematic view of reserves and resources of the Chuquicamata mine [15].

between models is the depth of the undercut and undercut span.

In the first, second, and third models, the undercut is located at the depths of 200, 800, and 1500 meters below the open-pit floor, respectively. The maximum undercut span for the first model is 100m and for other models, it is 125m. The block caving mining operation started when the open-pit mining operation was finished.

Figure 3 shows the geometry of the first model. The model was meshed using a 4-node mesh, as the boundary conditions of the model are shown in Figure 3. At the bottom boundary of the model, the displacement is fully constrained, and both the left and right sides of the model are constrained in the X direction. The model is under the force of gravity. The rock mass failure criterion in the numerical model is Mohr-Coulomb. The main input parameters used for the rock mass are summarized in Table 2.

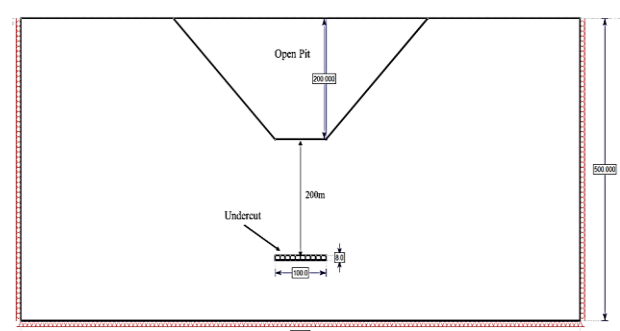

Figure 3. The geometry and boundary conditions of the numerical model.

4. Results and Discussion

Figure 4 illustrates the yield zone changes in each stage of undercutting in the first model. As it is obvious in the figure, the caving initiates in the span of 20 meters, and then it propagates upwards with the increase of the undercut span. The caving has not reached the pit floor until the undercut span is 90 meters for the depth of 200 meters. Therefore, the maximum undercut span can be 90 meters. In this span, the thickness of the crown pillar will be 32 meters.

Also, the displacement and strain contours in the last stage of undercutting are shown in Figure 5. This figure also shows that in order to ensure the stability of the pit, the crown pillar should remain at the

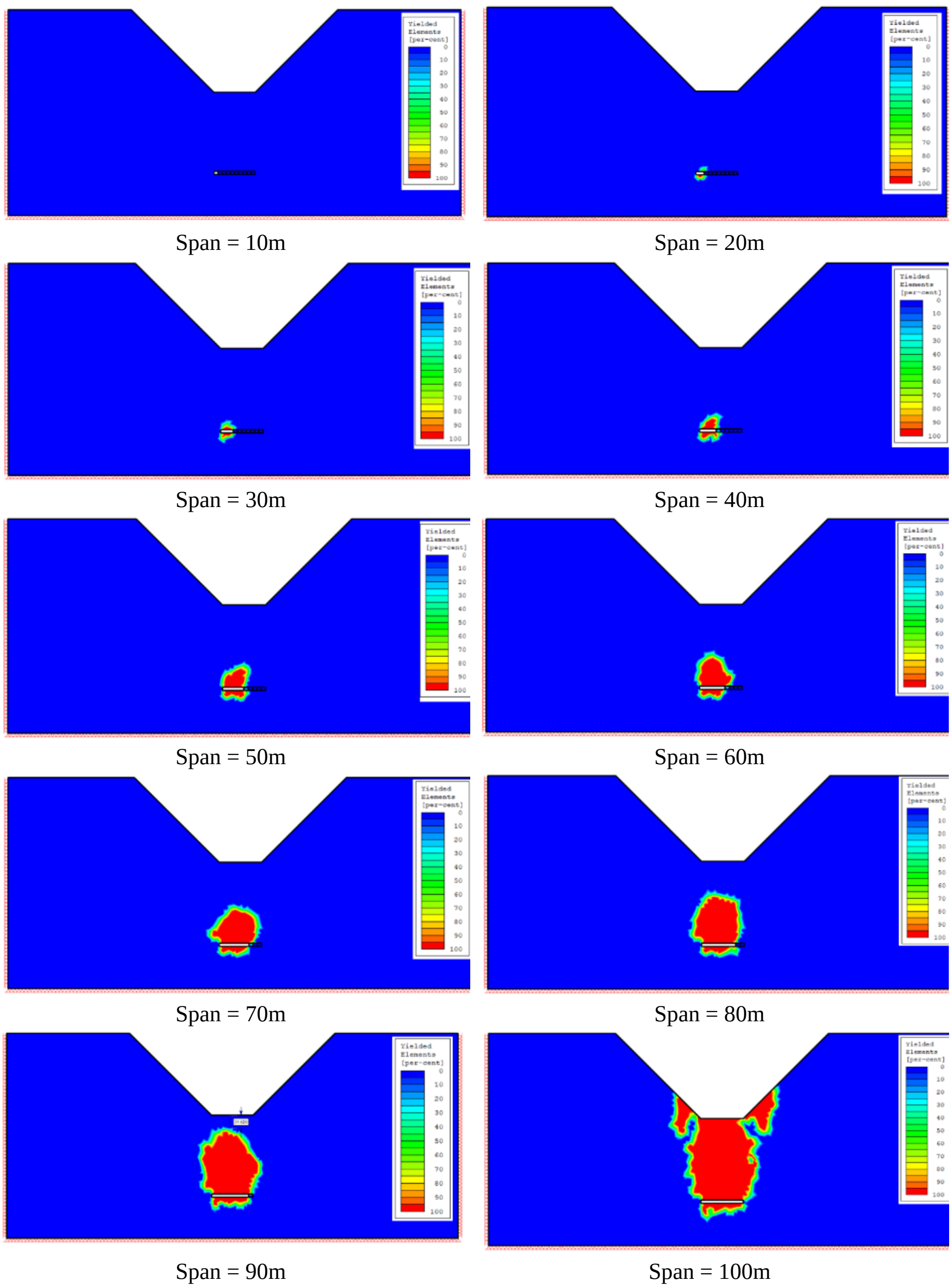

Figure 4. Yield zone in different stages of undercutting.

bottom of the pit with a thickness of 78 and 60 meters, respectively. By considering displacement and strain criteria, a conservative estimate for the thickness of the crown pillar will be obtained. Accordingly, a significant amount of ore will not be recovered. Therefore, the shear and tensile failure criterion is more suitable for this purpose.

Table 2. Input material parameters are used in numerical modelling [22].

Parameter	UCS (Intact Rock)	Mohr-Coulomb		Rock Mass Parameters		
		C	φ	σ_t	σ_{cm}	E_m
Unit	MPa	MPa	degree	MPa	MPa	GPa
Value	102	5.18	35.42	0.2	21.9	14.22

Figure 6 shows the changes in the shape of the yielded zone and the displacement contour at the maximum caving span before the caving reaches the pit floor. In this span, the thickness of the crown pillar will be 160 meters. In other words, the maximum usable span at a depth of 600 meters is equal to 125 meters. If the width of the span is larger than this value, the caving will reach the pit floor.

Figure 7 shows the changes in the shape of the yielded area and the displacement contour for the undercut at the depth of 1000 meters. At this depth, the maximum applicable caving span is equal to 135 meters. More than that, failure will happen in the pit floor. The thickness of the crown pillar, in this case, is 330 meters.

Figure 8 to Figure 10 depict the changes in crown pillar thickness, caving height, and the ratio of undercut span to crown pillar thickness in terms of depth, respectively. As it can be observed, with the increase in depth, the height of caving and the thickness of the crown pillar increase. With an increase in depth, the magnitude of in-situ stresses and consequently the induced stresses and the height of the caving zone increase. Also, for a slight change in the undercut span, a significant increase in the height of the caving zone will occur. Therefore, as the thickness of the crown pillar increases, the undercut span's ratio to the crown pillar's thickness decreases. At first, this decrease in the ratio has a steep slope, and then it becomes more gradual.

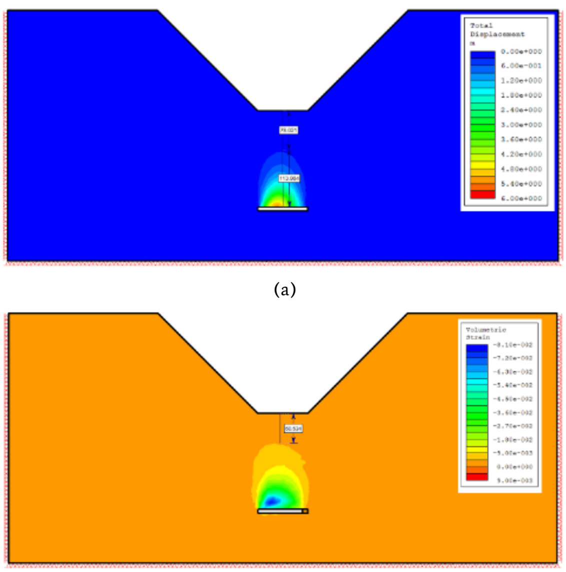

(a)

(b)

Figure 5. a) Displacement contours, and b) strain contours for the span of 100m at the depth of 200m

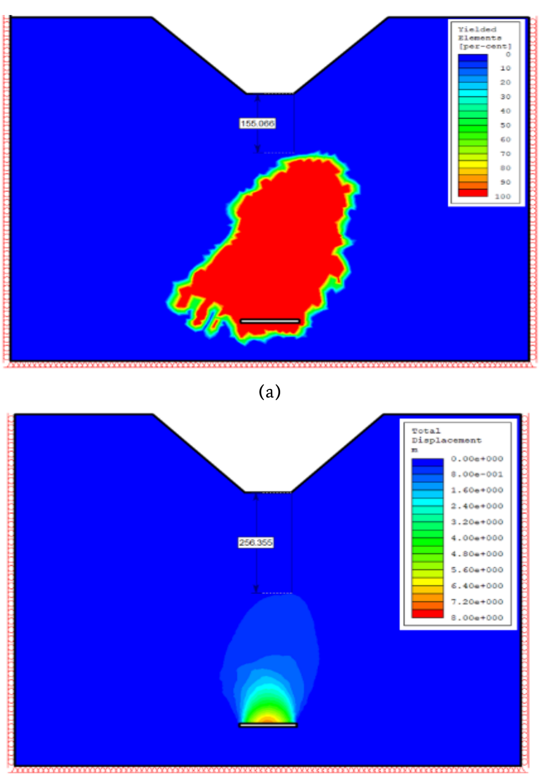

(a)

(b)

Figure 6. a) Yield zone contours, and b) displacement contours for the span of 125m at the depth of 600m.

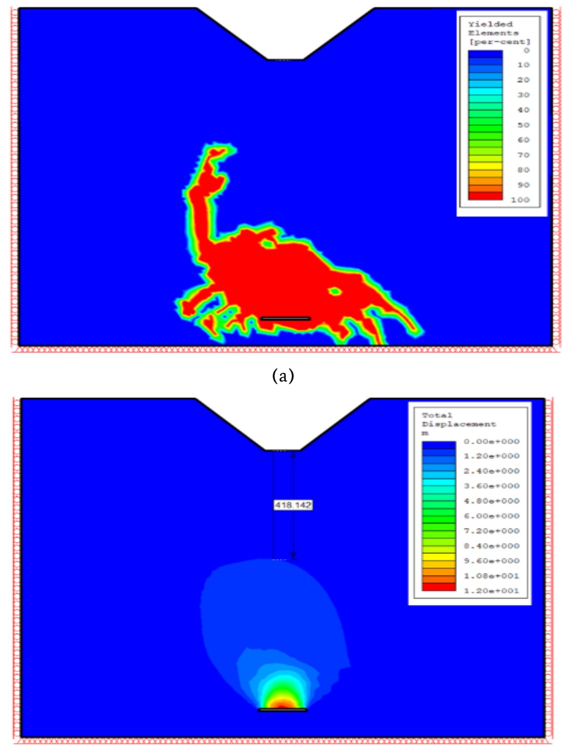

(a)

(b)

Figure 7. a) Yield zone contours, and b) displacement contours for the span of 125m at the depth of 1000m.

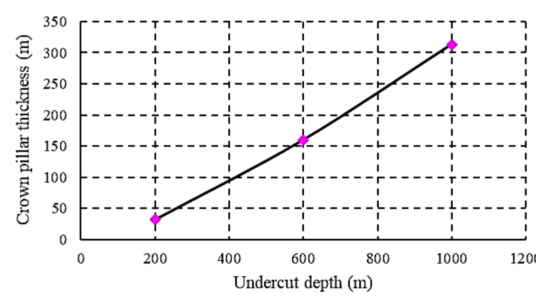

Figure 8. The diagram of crown pillar thickness based on the undercut depth.

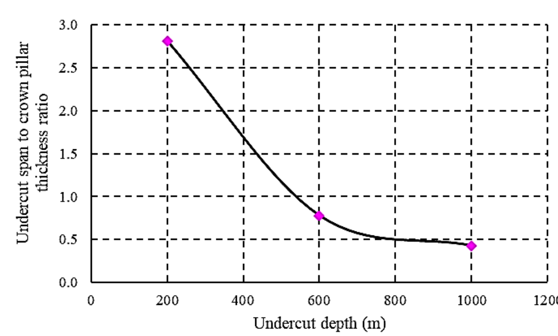

Figure 9. The diagram of Undercut span to crown pillar thickness ratio based on the undercut depth.

5. Conclusions

The knowledge of the crown pillar thickness between the pit bottom and the crown of the cave back has an impact on the stability analysis of the open-pit mine and calculation of the minable deposit from underground mine and cavability studies. Since this paper used numerical modelling to investigate the caving behavior under an

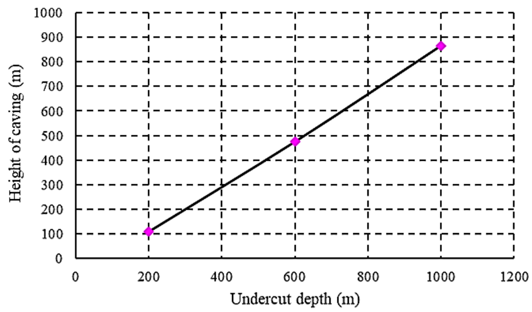

Figure 10. The diagram of caving height based on the undercut depth.

existing open-pit mine, the results are as follows:

(1) Numerical modelling showed that with an increase in the undercut depth, the magnitude of induced stresses on the top of the undercut increases. Stress concentration above the undercut causes yielding and consequently caving. The caving propagates upwards to the bottom of the pit.

(2) Controlling the width of the undercut span will prevent damage to the pit floor and instability in the floor and walls. On the other hand, to maximize the recovery, the undercut span should increase as much as possible.

(3) The height of the caving zone and the crown pillar thickness have a linear relationship with the undercut depth and increase with the increase in the undercut depth. For instance, with an increase in the undercut depth from 200 meters to 1000 meters, the crown pillar thickness and the caving zone height have increased by 281 meters and 755 meters, respectively.

(4) There is a logarithmic relationship between undercut depth and the ratio of undercut span to crown pillar thickness. As the undercut depth increases from 200 to 1000 meters, the ratio decreases by about 86%. In other words, with the increase in depth, the required thickness of the crown pillar increases.

Statements and Declarations

1. Funding

The authors declare that no funds, grants, or other support were received during the preparation of this manuscript.

2. Competing Interests

The authors have no relevant financial or non-financial interests to disclose.

3. Data Availability

The datasets generated during the current study are not publicly available due to not being published yet but are available from the corresponding author on reasonable request.

References

[1]. Alipenhani, B., Bakhshandeh Amnieh, H., & Majdi, A. (2022). Physical model simulation of block caving in jointed rock mass. *International Journal of Mining and Geo-Engineering*, *56*(4), 349–359. https://doi.org/10.22059/ijmge.2022.339663.594953

[2]. Alipenhani, B., Bakhshandeh Amnieh, H., & Majdi, A. (2023). Application of Finite Element Method for Simulation of Rock Mass Caving Processes in Block Caving Method. *International Journal of Engineering, Transactions A: Basics*, *36*(1), 139–151. https://doi.org/10.5829/ije.2023.36.01a.16

[3]. Alipenhani, B., Majdi, A., & Bakhshandeh Amnieh, H. (2022). Cavability assessment of rock mass in block caving mining method based on numerical simulation and response surface methodology. *Journal of Mining and Environment*, *13*(2), 579–606. https://doi.org/10.22044/jme.2022.11858.2176

[4]. Alipenhani, B., Majdi, A., & Bakhshandeh Amnieh, H. (2022). Determination of caving hydraulic radius of rock mass in block caving method using numerical modeling and multivariate regression. *Journal of Mining and Environment*, *13*(1), 217–233. https://doi.org/10.22044/jme.2022.11589.2149

[5]. Woo, K.-S., Eberhardt, E., Elmo, D., & Stead, D. (2013). Empirical investigation and characterization of surface subsidence related to block cave mining. *International Journal of Rock Mechanics and Mining Sciences*, *61*, 31–42. https://doi.org/10.1016/j.ijrmms.2013.01.015

[6]. Ren, F., Liu, Y., Cao, J., He, R., Fu, Y., Zhou, Y., & Liu, H. (2018). Prediction of the caved rock zones' scope induced by caving mining method. *PLoS One*, *13*(8), 16. https://doi.org/10.1371/journal.pone.0202221

[7]. Yang, G., Leung, A. K., Xu, N., Zhang, K., & Gao, K. (2019). Three-dimensional physical and numerical modelling of fracturing and deformation behaviour of mining-induced rock slopes. *Applied Sciences*, *9*(7), 1360–1375. https://doi.org/10.3390/app9071360

[8]. Flores, G., & Karzulovic, A. (2004). *Geotechnical guidelines for a transition from open pit to underground mining. Subsidence. ICS-II* (p. 78). Task 4, Technical Report.

[9]. Eberhardt, E., Stead, D., Elmo, D., Dunbar, S., Scoble, M., van As, A., Moss, A., Vyazmensky, A., Tollenaar, R., O'Connor, O. P., Eissa, H., & Sturzenegger, M. (2007). Transition from Surface to Underground Mining — Understanding Complex Rock Mass Interactions Through the Integration of Mapping, Monitoring and Numerical Modelling Data. *Proceedings of the International Symposium on Rock Slope Stability in Open Pit Mining and Civil Engineering, Perth, Australia*, 321–332. https://doi.org/10.36487/ACG_repo/708_19

[10]. Elmo, D., Vyazmensky, A., Stead, D., & Rance, J. (2008). Numerical analysis of pit wall deformation induced by block-caving mining: A combined FEM/DEM-DFN synthetic rock mass approach. *Proceedings of the 5th International Conference and Exhibition on Mass Mining, Lulea, Sweden*, 1073–1084.

[11]. Beck, D. A., Sharrock, G., & Capes, G. (2011). A coupled DFE-Newtonian cellular automata cave initiation, propagation and induced seismicity. *ARMA US Rock Mechanics/Geomechanics Symposium*, 9.

[12]. Xu, N., Zhang, J., Tian, H., Mei, G., & Ge, Q. (2016). Discrete element modeling of strata and surface movement induced by mining under open-pit final slope. *International Journal of Rock Mechanics and Mining Sciences*, *88*, 61–76. https://doi.org/10.1016/j.ijrmms.2016.07.006

[13]. Svartsjaern, M., Saiang, D., Nordlund, E., & Eitzenberger, A. (2016). Conceptual numerical modeling of large-scale footwall behavior at the Kiirunavaara mine, and implications for deformation monitoring. *Rock Mechanics and Rock Engineering*, *49*, 943–960. https://doi.org/10.1007/s00603-015-0750-x

[14]. Tegachouang, N. C., Bowa, V. M., Li, X., Luo, Y., & Gong, W. (2022). Study of the influence of block caving underground mining on the stability of the overlying open pit mine. *Geotechnical and Geological Engineering*, *40*(1), 165–173. https://doi.org/10.1007/s10706-021-01890-0

[15]. Brown, E. T. (2002). *Block Caving Geomechanics* (Vol. 1). Julius Kruttschnitt Mineral Research Centre.

[16]. Laubscher, D. H. (2000). *A Practical Manual on Block Caving*

(p. 525). https://www.resolutionmineeis.us/documents/laubscher-2000

[17]. Darling, P. (2011). *SME mining engineering handbook* (Vol. 1). SME.

[18]. Alipenhani, B., Bakhshandeh Amnieh, H., & Majdi, A. (2024). Evaluation of effective geomechanical parameters in rock mass cavability using different intelligent techniques. *International Journal of Mining and Geo-Engineering*. https://doi.org/10.22059/IJMGE.2024.369958.595133

[19]. Alipenhani, B., Jalilian, M., Majdi, A., Bakhshandeh Amnieh, H., & Khosravi, M. H. (2024). Determination of the caving zone height using numerical and physical modeling based on the undercutting method, joint dip, and spacing. *Journal of Mining and Environment*. https://doi.org/10.22044/jme.2024.13984.2609

[20]. Alipenhani, B., Majdi, A., & Bakhshandeh Amnieh, H. (2023). Investigating mechanical and geometrical effects of joints on minimum caving span in mass caving method. *International Journal of Mining and Geo-Engineering*, *57*(2), 223–229. https://doi.org/10.22059/IJMGE.2023.353554.595019

[21]. Alipenhani, B., Majdi, A., Amnieh, H. B., & Amini, E. (2024). Prediction of the height of caving zone above the undercut in block caving mining method. *Rock Mechanics Letters*, *1*(1), 31–36. https://doi.org/10.70425/rml.202401.5

[22]. Smolik, J. (2012). *Pre-feasibility Block Cave Mine Design—Iron Cap Deposit* (p. 182). Seabridge Gold Inc.